

The published version of the paper " W. Yang, E. Fortunati, F. Bertoglio, J. S. Owczarek, G. Bruni, M. Kozanecki, J. M. Kenny, L. Torre, L. Visai, D. Puglia (2018). Polyvinyl alcohol/chitosan hydrogels with enhanced antioxidant and antibacterial properties induced by lignin nanoparticles. Carbohydrate Polymers, 181, 275-284" is available at: <https://doi.org/10.1016/j.carbpol.2017.10.084>

1 **Polyvinyl alcohol/chitosan hydrogels with antioxidant and antibacterial properties**
2 **induced by lignin nanoparticles**

3
4 W. Yang¹, E. Fortunati¹, F. Bertoglio^{3,4,5}, J. S. Owczarek², G. Bruni⁶, M. Kozanecki², J. M.
5 Kenny¹, L. Torre¹, L. Visai^{3,5*}, D. Puglia^{1*}
6

7 ¹ *University of Perugia, Civil and Environmental Engineering Department, Materials Engineering Center, UdR*
8 *INSTM, Terni – Italy*

9 ² *Lodz University of Technology, Department of Molecular Physics, Lodz - Poland*

10 ³ *Molecular Medicine Department (DMM), Center for Health Technologies (CHT), UdR INSTM, University of*
11 *Pavia, Via Taramelli 3/B, 27100 Pavia, Italy*

12 ⁴ *Scuola Universitaria Superiore IUSS, Palazzo del Broletto-Piazza della Vittoria, 15, 27100 Pavia, Italy*

13 ⁵ *Department of Occupational Medicine, Toxicology and Environmental Risks, Istituti Clinici Scientifici Maugeri*
14 *S.p.A., IRCCS, Via S. Boezio, 28, 27100, Pavia, Italy*

15 ⁶ *Department of Chemistry, — Physical-Chemistry Section, University of Pavia, Viale Taramelli 16, 27100, Pavia,*
16 *Italy*

17
18
19
20
21 Weijun Yang, weijun.yang2012@gmail.com

22
23 Elena, Fortunati, elena.fortunati@unipg.it

24
25 Federico Bertoglio, federico.bertoglio01@ateneopv.it

26
27 Jan Owczarek, 164040@edu.p.lodz.pl

28
29 Giovanna Bruni, giovanna.bruni@unipv.it

30
31 Marcin Kozanecki, marcin.kozanecki@p.lodz.pl

32
33 Josè Maria Kenny, jose.kenny@unipg.it

34
35 Luigi Torre, luigi.torre@unipg.it

36
37 Livia Visai, livia.visai@unipv.it

38
39 Debora Puglia, debora.puglia@unipg.it
40

1 **Novel polyvinyl alcohol/chitosan hydrogels with antioxidant and antibacterial properties**
2 **induced by lignin nanoparticles**

3
4 W. Yang¹, E. Fortunati¹, F. Bertoglio^{3,4,5}, J. S. Owczarek², G. Bruni⁶, M. Kozanecki², J. M.
5 Kenny¹, L. Torre¹, L. Visai^{3,5*}, D. Puglia^{1*}
6

7 ¹ *University of Perugia, Civil and Environmental Engineering Department, Materials Engineering Center, UdR*
8 *INSTM, Terni – Italy*

9 ² *Lodz University of Technology, Department of Molecular Physics, Lodz - Poland*

10 ³ *Molecular Medicine Department (DMM), Center for Health Technologies (CHT), UdR INSTM, University of*
11 *Pavia, Via Taramelli 3/B, 27100 Pavia, Italy*

12 ⁴ *Scuola Universitaria Superiore IUSS, Palazzo del Broletto-Piazza della Vittoria, 15, 27100 Pavia, Italy*

13 ⁵ *Department of Occupational Medicine, Toxicology and Environmental Risks, Istituti Clinici Scientifici Maugeri*
14 *S.p.A., IRCCS, Via S. Boezio, 28, 27100, Pavia, Italy*

15 ⁶ *Department of Chemistry, — Physical-Chemistry Section, University of Pavia, Viale Taramelli 16, 27100, Pavia,*
16 *Italy*

17 **Corresponding authors:*

18 debora.puglia@unipg.it, Tel +39 0744 492916; Fax +39 0744 492950

19 livia.visai@unipv.it, Tel +39 0382 987725; Fax: +39 0382 423108
20

21 **Abstract**

22 Polyvinyl alcohol/chitosan (PVA/CH) hydrogels containing 1 and 3 wt % of lignin nanoparti-
23 cles (LNP) were prepared through a freezing-thawing procedure. Results from microstructural,
24 thermal and mechanical characterization of LNP based PVA/CH demonstrated that the lowest
25 amount of LNP (1 wt %) was beneficial, whereas the presence of agglomerates at higher LNP
26 content limited the effect. Moreover, a different swelling behaviour was observed for hydro-
27 gels containing LNP with respect of PVA/CH, due to the formation of a porous honey-
28 comb-like structure. A synergic effect of CH and LNP was revealed in terms of antioxidative
29 response by DPPH activity of migrated substances, whereas results from antimicrobial tests
30 confirmed LNP as effective against Gram negative bacteria (*E.Coli*) when compared to Gram
31 positive (*S.aureus* and *S. epidermidis*) strains. The obtained results suggested the possible use
32 of produced PVA/CH hydrogels incorporating LNP in many different sectors, such as drug
33 delivery, food packaging, wound dressing.

34
35 **Keywords:** polyvinyl alcohol, chitosan, lignin nanoparticles, hydrogels, antioxidative, an-
36 tibacterial
37
38

1 **1. Introduction**

2 Hydrogels have unique properties, as flexible approach in the synthesis phase, tuneable phys-
3 ical performance, desirable constituents and high biocompatibility. Specifically, their excel-
4 lent biocompatibility with the human tissue constructs and low irritation to the surrounding
5 tissues make them more attractive in different applications, as in the case of controlled drug
6 and protein delivery, tissue engineering and cosmeceutical (Slaughter, Khurshid, Fisher,
7 Khademhosseini, & Peppas, 2009). However, the poor mechanical properties of hydrogels af-
8 ter swelling limited its applications. In order to improve the mechanical properties of hydro-
9 gels, some methods has been taken into consideration, like physical blending, chemical modi-
10 fication by grafting, realization of interpenetrating polymer networks, and crosslinking meth-
11 od (J. M. Yang, Su, & Yang, 2004). Polyvinyl alcohol (PVA), a water soluble and semicrys-
12 talline plastic, has been widely utilized in preparation of hydrogels, because of its excellent
13 properties, including solvent resistance, mechanical performance, high hydrophilicity and bi-
14 ocompatibility (Kubo & Kadla, 2003; Liu, Chen, Liu, Bai, & Wang, 2014). In addition, it can
15 be easily mixed with some other polymers already widely considered for applications in the
16 cited sectors, one of them is the chitosan (CH), a non-toxic cationic polysaccharide isolated
17 from some natural crustacean shells, like crab and shrimp. CH is a copolymer of
18 2-glucosamine and N-acetyl-2-glucosamine units, wherein the former constitutes a major
19 fraction of the biopolymer chain. Chitosan has been widely studied for biosensors, tissue en-
20 gineering, separation film, water treatment, due to its preferable properties as antioxidant, an-
21 tibacterial agent, and for its good biocompatibility and biodegradability (Crini & Badot, 2008;
22 Kumar, 2000; Rinaudo, 2006). However, some disadvantages such as dissolution in highly
23 acidic solution, low surface area, high cost, poor thermal and mechanical properties restrict its
24 applications. To make up for the advantages and disadvantages of both PVA and CH, hydro-
25 gels based on PVA/CH blends have been developed. Nowadays, PVA/CH blend hydrogels
26 have been reported to be used for the controlled release of drugs, because of their low toxicity
27 and high biocompatibility. Kim et al. (S. J. Kim, Park, & Kim, 2003) reported about PVA/CH
28 hydrogels prepared by UV irradiation, which exhibited high dependence of swelling on pH
29 and temperature. Abdel-Mohsen et al. (Abdel-Mohsen, Aly, Hrdina, Montaser, & Hebeish,
30 2011) also concluded that the swelling of these hydrogels, synthesized by freeze-thawing for

1 the release of a model antibiotic, sparfloxacin, is pH dependent. In the meanwhile, their hy-
2 drogels displayed a positive effect towards the inhibition of Gram-positive and Gram-negative
3 bacterial growth. Indeed, the release of sparfloxacin also relies on both pH and temperature.
4 Yang et al. (J. M. Yang, Su, & Yang, 2004) prepared PVA/CH hydrogel membranes in vari-
5 ous ratios and treated them with formaldehyde as crosslinking agent: their results showed that
6 thermostability of the hydrogel membranes was enhanced, while PVA crystallinity decreased.
7 Moreover, it was demonstrated that CH content variation and treatment with formaldehyde
8 has no influence in the antibacterial assessment. Yang et al (X. Yang, Liu, Chen, Yu, & Zhu,
9 2008) also reported about the use of PVA/CH hydrogels for wound dressing, obtained by
10 γ -irradiation combined with freeze-thawing. They found that hydrogels obtained by irradiation
11 plus freeze-thawing show larger swelling capacity and mechanical strength, higher thermal
12 stability, lower water evaporation rate, and are less turbid than those made by pure
13 freeze-thawing and freeze-thawing followed by irradiation. The same hydrogels presented al-
14 so good antibacterial activity against *Escherichia coli*. Zu et al. (Zu et al., 2012) synthesized
15 PVA/CH hydrogels by using glutaraldehyde as crosslinking agent, with the aim of testing
16 their use for transdermal drug delivery of nano-insulin. The hydrogel showed good mechani-
17 cal and thermal properties, along with a high permeation rate of nano-insulin ($4.421 \text{ ug}/(\text{cm}^2$
18 $\text{h})$), suggesting high potential use of these hydrogels for non-invasive transdermal drug deliv-
19 ery system in diabetes chemotherapy.

20 Lignin is the second most abundant natural polymer next to cellulose, which makes up
21 20-30% of the cell walls of plants. It has always been utilized in low-value fields, for example
22 heat and electricity generation. Nowadays, more researchers realise that its abundance could
23 potentially resolve some environmental problems if we could successfully translate it into
24 higher value material, including its use as antioxidant, UV absorbent, antimicrobial agent, re-
25 inforcement agent, carbon precursor and biomaterial for tissue engineering and gene therapy
26 (Kai et al., 2016; Thakur, Thakur, Raghavan, & Kessler, 2014). A recent study reported the
27 use of nanoparticles combining chitosan and lignosulfonates for cosmetic and biomedical uses
28 (S. Kim et al., 2013). A greater stability to lysozyme degradation, antimicrobial activity and
29 biocompatibility with human cells were concluded upon lignosulfonates incorporation into
30 chitosan nanoparticles. No examples can be found where the antimicrobial activity of chi-

1 tosan/PVA based blend was tested in presence of lignin, which has been demonstrated to have
2 inherent antimicrobial and antioxidant capabilities at the nanoscale. In this study, we synthe-
3 sized PVA/CH hydrogels through a simple freeze-thawing approach and we aimed to study
4 how different amount of lignin nanoparticles (LNP), incorporated in PVA/CH hydrogels,
5 could modify not only blend microstructure, but also swelling, thermal, mechanical, antibac-
6 terial and antioxidant behaviour of reference blend.

7

8 **2. Experimental section**

9

10 *2.1 Materials*

11 Polyvinyl alcohol (PVA) (M_w 124–146 kg mol⁻¹, 99% hydrolyzed), a synthetic and biode-
12 gradable polymer produced by the hydrolysis of polyvinyl acetate, was supplied by Sig-
13 ma–Aldrich[®] (Italy). High molecular weight chitosan (CH), (practical grade, Batch
14 MKBB0585, degree of deacetylation >77%, viscosity: 1220 cPs, 1.61×10^5 Da), was supplied
15 by Sigma–Aldrich[®] (Italy).

16 Pristine lignin, obtained as bio-residue of conversion of *Arundo donax L.* biomass to bioetha-
17 nol in a steam explosion pre-treatment, followed by enzymatic reactions and filtration, was
18 supplied by CRB (Centro Ricerca Biomasse, University of Perugia) (Cotana et al., 2014).

19 Lignin nanoparticle (LNP) suspension was prepared from pristine lignin by hydrochloric aci-
20 dolysis, as presented in our previous work (Weijun Yang, Kenny, & Puglia, 2015). All the
21 chemical reagents were supplied by Sigma–Aldrich[®] and used as received.

22

23 *2.2 Methods*

24 *2.2.1 Preparation of binary PVA/CH and ternary PVA/CH/LNP nanocomposite hydrogels*

25 PVA/CH (90/10) hydrogel was prepared according to the following steps: PVA was diluted in
26 deionized water at 20% (wt/v) under magnetic stirring at 90 °C for 4 h, while chitosan was
27 dissolved in water with glacial acetic acid (1% v/v) under magnetic stirring at 40 °C for 12 h.
28 According to the designed blending ratio, the mixed solutions of chitosan and PVA were
29 sonicated (Vibracell 75043, 750W, Bioblock Scientific) for 5 min at 40% of amplitude and
30 homogeneous solutions were obtained and poured into a Petri dish cover by a Teflon[®] sheet.

1 After that, the poured material was kept at -30°C for 18 hours to freeze and then exposed at
2 25°C to thaw for 4 hours to complete one cycle. The hydrogels were prepared by repeating
3 four times the above freezing/thawing cycles and, with the freezing step exceeded 18 h in the
4 final cycle. In order to eliminate the free polymer molecules not incorporated into the cross-
5 link regions and the free ions, all the hydrogels were soaked in pure water for several times.
6 PVA/CH/LNP ternary nanocomposite hydrogels containing 10 wt % of chitosan and 1 and 3
7 wt % of LNP were also prepared, by using the following protocol: PVA was diluted in deion-
8 ized water at 20% (wt/v) under magnetic stirring at 90°C for 4 h and a specific amount of the
9 aqueous dispersion of LNP was added in order to obtain the selected percentage of LNP re-
10 spect to the PVA matrix. The mixture was then sonicated (Vibracell 75043, 750W, Bioblock
11 Scientific) for 5 min at 40 % of amplitude. Chitosan was separately dissolved in water with
12 glacial acetic acid (1% v/v) under magnetic stirring at 40°C for 12 h and then added to the
13 PVA/LNP solution previously obtained. The final mixture was again sonicated for 5 min at
14 40% of amplitude and cast into a Petri dish cover by a Teflon[®] sheet. Five consecutive freeze
15 (-30°C , 18 hour) and thaw (room temperature, 4 h) cycles, with a longer final freeze cycle,
16 were also considered in this case.

17

18 *2.2.2 Morphological analysis*

19 The microstructure of hydrogel cross-sections was observed by using a Field Emission Scan-
20 ning Electron Microscope, FESEM, Supra 25-Zeiss. Specimens were cryo-fractured by im-
21 mersion in liquid nitrogen and mounted on copper stubs perpendicularly to their surface.
22 Samples were gold coated and observed by using an accelerating voltage of 4 kV.

23

24 *2.2.3 Differential scanning calorimetry (DSC)*

25 Hydrogel samples of about 3 mg were tested by using a differential scanning calorimeter
26 (DSC, TA Instrument, Q200). Measurements were carried out under nitrogen flow in the
27 temperature range from -25°C to 220°C at a heating rate of $10^{\circ}\text{C}/\text{min}$. After a first heating
28 step, cooling and second heating were performed. Data were recorded both during the cooling
29 and second heating steps. The glass transition temperature (T_g) was taken as the inflection
30 point of the specific heat increment at the glass-rubber transition, while the melting tempera-

1 ture (T_m) and melting enthalpy (ΔH_m) were determined during the cooling and the 2nd heating
2 scan, respectively. Three samples were used to characterize each material.

4 2.2.4 Thermogravimetric analysis (TGA)

5 TGA tests were carried out using a thermo gravimetric analyzer (TGA, Seiko Exstar 6300).
6 The samples, approximately 3 mg, were heated from 30 to 600 °C at a heating rate of
7 10°C/min under nitrogen atmosphere. The peak values temperatures and 20% of weight loss
8 temperature ($T_{20\%}$) were obtained from derivative thermogravimetric (DTG) data, along with
9 the residual weight at 600 °C.

11 2.2.5 Dynamic mechanical thermal analysis (DMTA)

12 Dynamic mechanical properties of hydrogel samples were measured using ARES N2 instru-
13 ment (Reometric Scientific) in torsion mode on a plate with a diameter of 8 mm. The storage
14 (G'), loss modulus (G'') and viscosity ($\text{Log } \eta$) values were obtained at a constant temperature
15 of 25 °C, strain amplitude of 1.0% and over a frequency range from 0.1 to 100 Hz.

17 2.2.6 Swelling studies

18 The swelling behavior of the nanocomposite hydrogels was measured in water (pH = 7.0) at
19 25 °C. The swelling ratio (SR, %) for each sample was calculated by applying the Eq. (1):

$$20 \quad SR = \frac{M_s - M_D}{M_s} \times 100 \quad (1)$$

21 where M_s and M_D are the hydrogel masses in the swollen and in the dry state, respectively. All
22 measurements were repeated four times.

24 2.2.7 Antiradical activity of migrating substances

25 DPPH radical scavenging activity for PVA/CH and ternary PVA/CH/LNP hydrogels contain-
26 ing different amount of lignin nanoparticles was determined according to the method pro-
27 posed by Byun et al. (Chernoberezhskii, Atanesyan, Dyagileva, Lorentsson, & Leshchenko,
28 2002) and Domenek et al. (Domenek, Louaifi, Guinault, & Baumberger, 2013) with a slight
29 modification. Hydrogel (0.1 g) was cut into small pieces and immersed in 2 mL of methanol

1 for 24 h at ambient temperature. The supernatant obtained was analyzed for evaluation of
2 DPPH radical scavenging activity: methanol extract (1 mL) was mixed with 1 mL of DPPH in
3 methanol (50 mg L⁻¹), resulting in a 25 mg L⁻¹ DPPH concentration solution. The mixture was
4 maintained at room temperature in the dark for 60 min. The absorbance was measured at 517
5 nm using a UV-Vis spectrometer (Varian, Cary 4000). The mixture solution of methanol ex-
6 tracted from neat PVA and DPPH methanol was used as control. DPPH radical scavenging
7 activity was calculated by using Equation 2, where A_{sample} was the absorbance of sample and
8 A_{control} was the absorbance of the control.

$$(RSA, \%) = \left[\frac{A_{control} - A_{sample}}{A_{control}} \right] * 100 \quad (2)$$

10

11 2.2.8 Antimicrobial tests: bacterial strain culture conditions and viability assays.

12 *Escherichia coli* RB (*E. coli* RB), *Staphylococcus aureus* 8325-4 (*S. aureus* 8325-4) and
13 *Staphylococcus epidermidis* RP62A (*S. epidermidis* RP62A) were used in this study. The
14 former was used as main representative of Gram negative bacteria, the latter two instead as
15 representatives of Gram positive bacteria. *E. coli* RB was kindly provided by the “Istituto
16 Zooprofilattico di Pavia” (Italy) whereas *S. aureus* 8325-4 and *S. epidermidis* RP62A were
17 kindly supplied by Timothy J. Foster (Department of Microbiology, Dublin, Ireland). *E. coli*
18 RB was routinely grown in Luria Bertani Broth (LB) (Difco, Detroit, MI, USA), *S. aureus*
19 8325-4 in Brian Heart Infusion (BHI) (Difco) and *S. epidermidis* RP62A in Tryptic Soy Broth
20 (TSB) (Difco) overnight under aerobic conditions at 37 °C, 200 rpm (Certomat[®] BS-T,
21 B.Braun Biotech International). To evaluate the antimicrobial activity of the generated hy-
22 drogels in planktonic conditions, the overnight cultures were diluted in fresh appropriate me-
23 dium and 150µL of diluted bacterial suspension were deposited on sterilized hydrogels placed
24 at the bottom of a 96-well flat-bottom polystyrene tissue culture plates (TCPs) well. 5 x 10⁴
25 bacteria/150 µL suspensions, obtained by comparing the O_{D600} of the overnight culture with a
26 standard curve correlating O_{D600} to cell number, were used to test the antibacterial activity at
27 37 °C for 24 hours. The samples were then incubated at 37 °C for 24 hours in static conditions.
28 Similarly, TCP empty wells were incubated with the same bacterial suspension at the same
29 temperature and time and used as positive control. At the end of the culturing period, the bac-

1 terial viability was assayed through the quantitative
2 3-[4,5-dimethylthiazol-2-yl]-2,5-diphenyltetrazoliumbromide (MTT) (Sigma Aldrich[®], StLou-
3 is, MO, USA) test, as previously reported (Yalcinkaya et al., 2017). Briefly, this colorimetric
4 assay measures dehydrogenase activity, as an indicator of the metabolic state of the cells. Af-
5 ter the indicated culturing times, bacterial suspensions were transferred to a new plate and cell
6 viability assessed. 5 mg/mL of MTT solution, dissolved in PBS (0.134 M NaCl, 20mM
7 Na₂HPO₄, 20 mM NaH₂PO₄), was used as stock solution and the working concentration was
8 0.5mg/mL. Bacteria were incubated in the presence of MTT solution at 37 °C for 3 hours.
9 Upon presence of viable cells, reduction of MTT salt results in purple insoluble formazan
10 granules. These precipitates were dissolved through acidified 2-propanol (0.04 N HCl). The
11 result was recorded through an iMark[®] Microplate Absorbance Reader (Bio-Rad) at 562 nm
12 with the reference wavelength set at 655 nm. Bacterial survival was expressed as percentage
13 of the number of bacteria survived on the generated hydrogels to number of bacteria grown on
14 TCP wells. Experiments were performed twice with triplicate samples.

15

16 2.2.9 Scanning electron microscopy (SEM) analysis.

17 Images of *E. coli* RB, *S. aureus* 8325-4 and *S. epidermidis* RP62A grown on LNP-enriched
18 PVA/CH hydrogels were prepared essentially as already reported (Yalcinkaya et al., 2017).
19 Briefly, all strains used in this study were incubated on previously sterilized hydrogels for 24
20 hours at 37°C. As a control, a Thermanox[™] coverslip (Nunc[™]) was used to deposit both
21 bacterial cells. Following incubation, samples were washed carefully with sterile water and
22 fixed with 2.5% (v/v) glutaraldehyde in 0.1 M Na-cacodylate buffer, pH 7.2, for 1 h at + 4 °C.
23 After additional washing with cacodylate buffer, the samples were dehydrated using increas-
24 ing concentrations of ethanol (25, 50, 75%) for 5 min and final two washes of 10 minutes in
25 96% ethanol. The samples were then lyophilized for 6 hours using an Emitech K-850 appa-
26 ratus, placed on a mounting base and sputter coated with gold (300 nm). Analysis was per-
27 formed using a Zeiss EVO-MA10 scanning electron microscope (Carl Zeiss, Oberkochen,
28 Germany).

29 2.2.10 Biofilm formation and viability analysis

1 Since *S. epidermidis* RP62A is a biofilm producer strain, we explored whether the generated
2 hydrogels were able to inhibit biofilm formation. To induce biofilm formation, overnight
3 grown bacteria were diluted 1:200 in TSB-medium containing 0.25% glucose as previously
4 described (Pallavicini et al., 2014; Saino et al., 2010; Sbarra et al., 2009; Taglietti et al.,
5 2014) . An aliquot 150µl of diluted bacterial suspension was deposited on each hydrogel and
6 incubated for 24 hours at 37°C. As positive control, TCPS wells were incubated with the
7 same amount of diluted bacterial suspension at the same incubation conditions. The viability
8 of *S. epidermidis* was evaluated as described above through MTT test after mechanical dis-
9 ruption of the biofilm. The results of the TCPS wells (control) were set to 100%. The experi-
10 ments were performed twice with triplicate samples.

11

12 **3. Results and discussion**

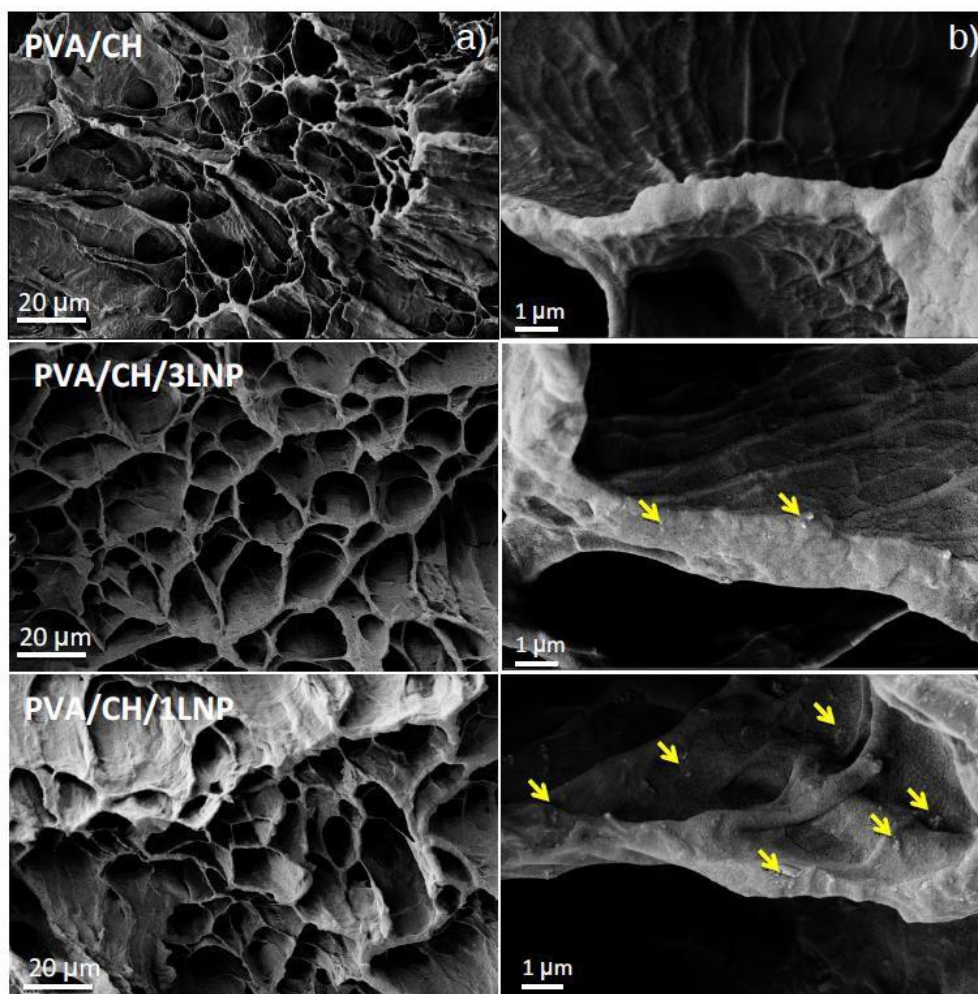
13

14 *3.1 Microstructure of produced hydrogels*

15 The morphologies of the freeze-dried hydrogels containing different amount of LNP are
16 shown in **Figure 1a**.

17 The PVA/CH hydrogel has an interconnecting porous structure, with macrovoids whose walls
18 are rough, whereas a porous honeycomb-like structure is shown for the hydrogels containing
19 LNP. It was supposed that the well dispersed lignin nanoparticles could serve as nucleation
20 agents (Lee et al., 2005), in the meanwhile, the hydrophobic nature of lignin and strong inter-
21 action between PVA/CH molecules and LNP prevents the PVA molecules from moving and
22 dissolving into the water, resulting in promoting the crosslinking effect (Xia, Yih, D'Souza, &
23 Hu, 2003). Consequently, more uniform and higher quantity of pore microstructures formed.
24 The pore diameter of PVA/CH/1LNP and PVA/CH/3LNP hydrogels is about 10-20 µm,
25 which indicates a good accessibility of water into the amorphous regions of the hydrogels.
26 This result demonstrates that LNP had a role in the formation of pores for the PVA/CH hy-
27 drogel. To further magnify the studied hydrogels, some LNP aggregates (arrows) could be
28 seen on the pore-wall surface in PVA/CH/1LNP and PVA/CH/3LNP hydrogels, more visible
29 in PVA/CH/3LNP system (**Figure 1b**).

30

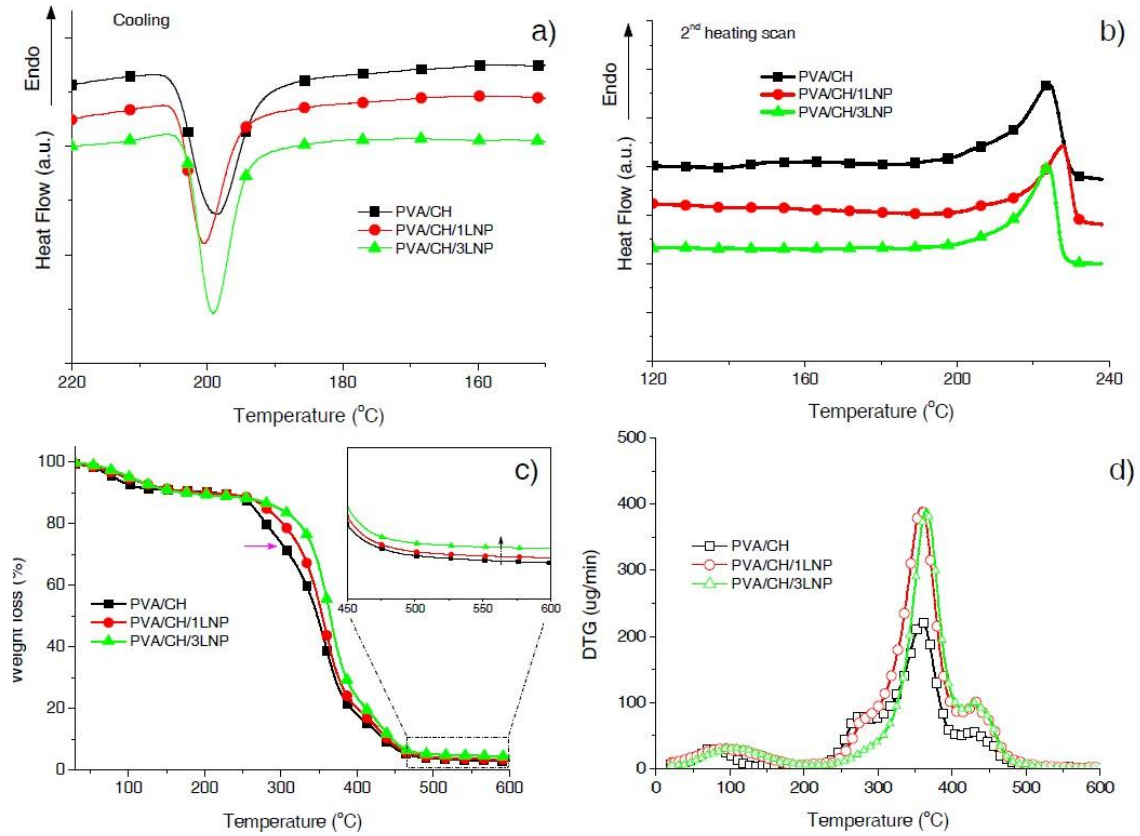


1 **Figure 1:** Morphologies of freeze-dried hydrogels containing different amount of LNP (a) and
 2 magnification of LNP aggregates (b).
 3

4
 5 *3.2 Differential scanning calorimetry*

6 DSC analysis was conducted to analyze the thermal properties of PVA/CH binary and ternary
 7 nanocomposite hydrogels containing LNP. The values of thermal parameters obtained in the
 8 cooling and second heating scans for all samples are summarized in **Table 1**, while DSC
 9 cooling and 2nd heating curves are reported in **Figure 2(a-b)**. A single composition-dependent
 10 glass transition temperature (T_g) is indicative of blend miscibility, even in presence of lignin
 11 nanoparticles. The addition of the LNP did not change the crystallization temperature of
 12 PVA/CH binary hydrogel, but lead to ΔH_m increase from 42.8 (PVA/CH) to 53.6 J/g
 13 (PVA/CH/1LNP), indicating that higher crystalline region was achieved and enhanced ther-
 14 mal stability has been achieved by adding LNP. PVA is a semicrystalline polymer bearing
 15 plenty of hydroxyl groups which form inter- and intra-molecular hydrogen bonds. Since LNP
 16 also have a lot of hydroxyl groups in their structures, strong molecular interactions (hydrogen

1 bonding or dipole-dipole interactions) between polymer and LNP can be expected (Hu, Ye,
 2 Tang, Zhang, & Zhang, 2016; Kubo & Kadla, 2003; Ye, Jiang, Hu, Zhang, & Zhang, 2016).
 3 However, addition of 3 wt % did not further increase the ΔH_m , the result could be understood
 4 when taking into account the abundant LNP agglomerates detected by SEM.



5
 6 **Figure 2:** DSC cooling (a) and 2nd heating curves (b) for PVA/CH hydrogels containing dif-
 7 ferent amount of LNP; TG (c) and DTG curves (d) of pure PVA binary and ternary system
 8 hydrogels with different LNP loading.

9
 10 **Table 1:** DSC and TGA thermal parameters of PVA/CH blend and PVA/CH/LNP hydrogel
 11 ternary systems

| | T_g (°C) | T_g (°C) | T_m (°C) | ΔH_m (J/g) | Peak 1 (°C) | Peak 2 (°C) | Peak 3 (°C) | $T_{20\%}$ (°C) | Residue at 600°C (%) |
|--------------------|---------------|---------------|---------------|-----------------------|-------------------|-------------------|-------------------|--------------------|-------------------------------|
| PVA/CH | - | - | 225.0±1.1 | 42.8±0.5 | 77.3 | 273.8 | 359.6 | 280.5 | 2.9 |
| PVA/CH/1LNP | 73.6±2.0 | 73.6±2.0 | 226.9±1.2 | 53.6±0.0 | 89.6 | 275.4 | 359.2 | 302.5 | 3.5 |
| PVA/CH/3LNP | 74.5±2.1 | 74.5±2.1 | 224.4±1.0 | 48.0±1.0 | 106.5 | - | 365.5 | 324.1 | 4.5 |

13 **3.3 Thermogravimetric analysis**

14 TG and DTG curves of pure PVA binary and ternary hydrogels were recorded in order to in-

1 investigate the effect of LNP loading on the thermal degradation behaviour of resulted compo-
2 sites (**Figure 2c-d**). The peak values of DTG and the residual weight at 600 °C, were also
3 summarized in **Table 1**. The degradation progress was divided into four steps: 1) the small
4 weight loss (peak 1) at 75-100 °C (about 10%) is due to the loss of adsorbed, bound water and
5 residual acetic acid; 2) The weight loss (peak 2) at 200-300 °C was attributed to the initial
6 thermal decomposition of CH and PVA; 3) the maximum decomposition range between 300
7 and 400 °C (peak 3) could be attributed to a complex degradation process of PVA and CH,
8 including the dehydration of the saccharides rings and the depolymerization of the acetylated
9 and deacetylated units of the polymer (J. M. Yang, Su, Leu, & Yang, 2004); 4) weight loss at
10 400-450 °C (peak 4) is related to the thermal degradation event of some by-products generat-
11 ed by PVA (Bonilla, Fortunati, Atarés, Chiralt, & Kenny, 2014; Chen, Wang, Mao, Liao, &
12 Hsieh, 2008). Evidently, with increasing dose of LNP from 0 to 3 wt %, the peak 1 shifted
13 from 77.3 up to 106.5 °C: this effect can be attributed to the pore-forming effect of LNP in
14 PVA/CH hydrogel, which efficiently delayed the removal of water and residual acetic acid.
15 Similar results were observed in our previous study with wheat gluten in presence of glycerol
16 (Weijun Yang et al., 2015). Interestingly, the peak 2 became less visible when 1 wt % of LNP
17 was used, and disappeared when 3 wt% of LNP was added, confirming the delayed decompo-
18 sition process of PVA and CH due to the addition of LNP. Furthermore, the $T_{20\%}$ also dra-
19 matically rose from 280.5 to 324.1 °C, along with increase in the weight residue at 600 °C
20 from 2.9 to 4.5 %.

21

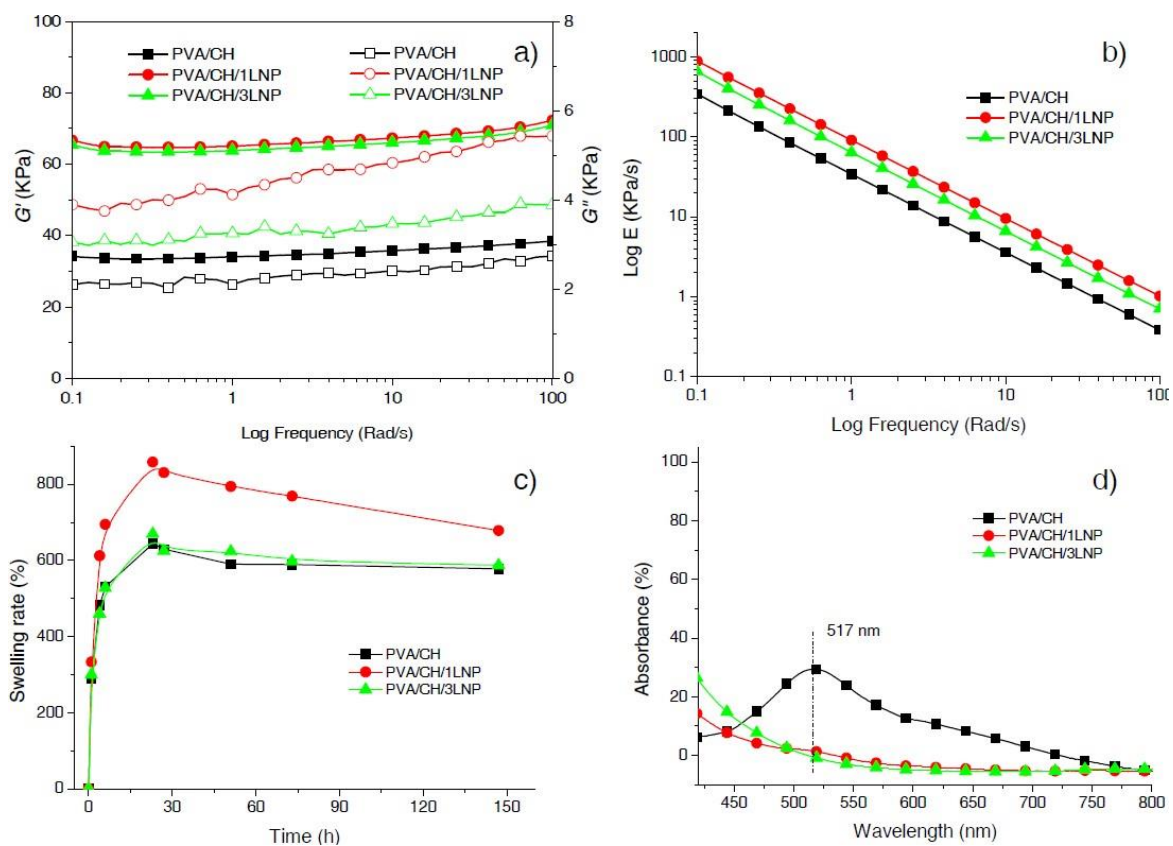
22 *3.4 Dynamic mechanical thermal analysis*

23 **Figure 3a-b** and **Table 2** show the storage modulus (G'), loss modulus (G'') and viscosity
24 ($\log \eta$) values versus scan frequency for various hydrogel samples. The PVA/CH shows the
25 lowest G' , G'' and viscosity values in all the frequency range. After the addition of 1 wt % of
26 LNP, the G' , G'' and viscosity increased from 34.8 KPa, 1.6 KPa and 34.9 KPa's to 63.4 KPa,
27 4.1 KPa and 63.5 KPa's at 1 Hz frequency, increasing by 82.2, 156.3 and 81.9 %, respectively.
28 The viscosity of the studied hydrogels decreased linearly with the increase of the frequency,
29 which was in consistence with previous results (Tang, Du, Hu, Shi, & Kennedy, 2007).

30

1 **Table 2:** G' and G'' values for PVA/CH blend and PVA/CH/LNP hydrogel ternary systems at
 2 two different frequencies

| Materials | G' (KPa) | | G'' (KPa) | | η (KPa \cdot s) | |
|-------------|----------------|----------------|---------------|---------------|------------------------|---------------|
| | 1 | 10 | 1 | 10 | 1 | 10 |
| PVA/CH | 34.8 \pm 0.8 | 36.3 \pm 0.5 | 1.6 \pm 0.5 | 1.9 \pm 0.5 | 34.9 \pm 5.7 | 3.6 \pm 0.1 |
| PVA/CH/1LNP | 63.4 \pm 8.0 | 64.3 \pm 8.0 | 4.1 \pm 0.8 | 4.8 \pm 1.0 | 63.5 \pm 10.0 | 6.4 \pm 1.5 |
| PVA/CH/3LNP | 62.2 \pm 3.7 | 64.8 \pm 3.4 | 3.1 \pm 0.7 | 3.5 \pm 0.7 | 62.3 \pm 3.6 | 6.5 \pm 0.3 |



6 **Figure 3:** Curves for Storage modulus (G'), loss modulus (G'') (a) and viscosity (Log η) (b)
 7 vs. frequency for PVA/CH hydrogels containing different amount of LNP; swelling behaviour
 8 of pure PVA binary and ternary system hydrogels with different LNP loading (c) and antioxi-
 9 dant response of migrating substances for different nanocomposite hydrogels directly im-
 10 mersed into the methanol solution for 24 h (d).

11
 12
 13 This result demonstrates that LNP could efficiently enhance the mechanical properties of
 14 PVA/CH hydrogel, which may due to the strong interactions between PVA/CH and LNP.
 15 Although the PVA/CH and lignin are immiscible in the bulk, the results showed the existence

1 of some specific intermolecular interaction (like hydrogen bonding or dipole-dipole interac-
2 tions) between them.

3 The same results were also confirmed by Korbag et al. (Korbag & Mohamed Saleh, 2016),
4 that used nuclear magnetic resonance and FTIR spectroscopy techniques. Recently, Ye et al.
5 (Ye et al., 2016) and Hu et al. (Hu et al., 2016) also found that PVA/lignosulfonate compo-
6 sites had preferable mechanical properties than pure PVA, due to the primary rigidity of
7 nanolignin structures and the formation of strong hydrogen bonds. However, when the load-
8 ing of LNP rose up to 3 wt %, the G' , G'' and $\text{Log } \eta$ shows steady even slightly decline with
9 respect to PVA/CH/1LNP hydrogel. This result could be responsible for the abundant for-
10 mation of LNP aggregates on the surface of hydrogels (Figure 1b).

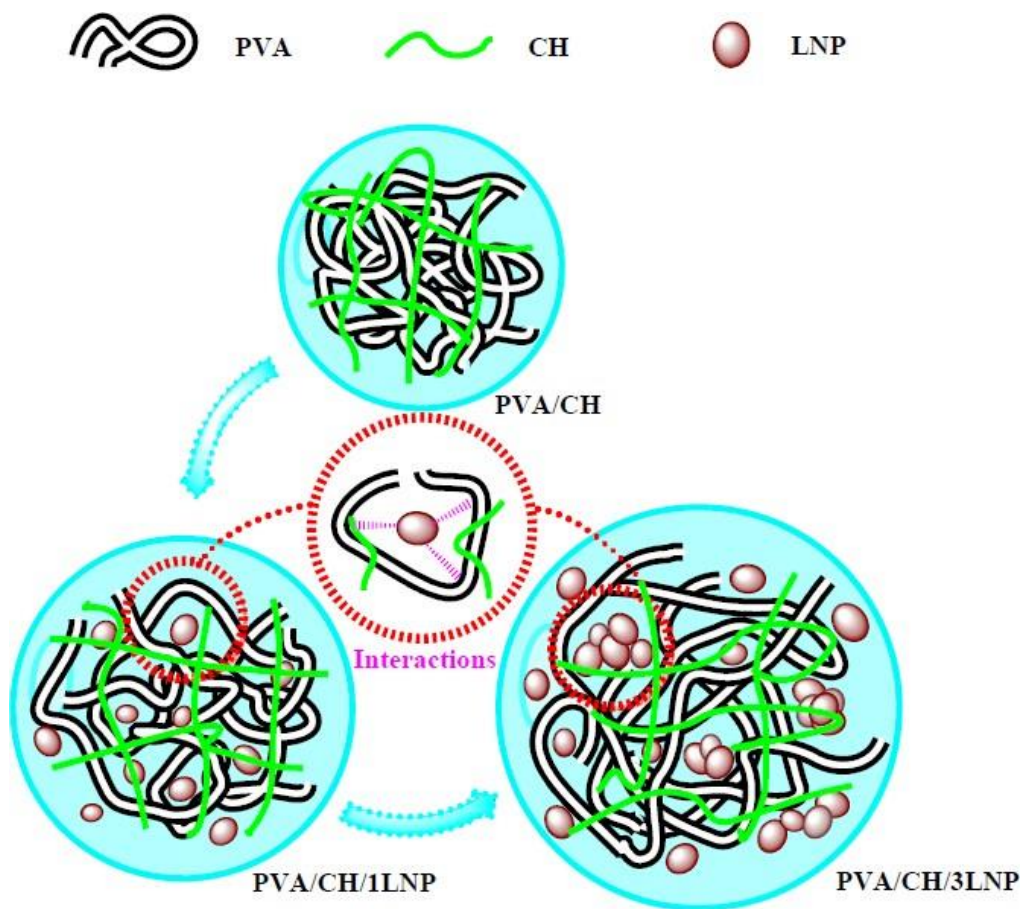
11

12 *3.5 Swelling behavior*

13 PVA/CH hydrogels have lots of hydrophilic groups, which show high accessibility to water,
14 but these polymer networks can be avoided dissolving in water due to the formed chemical or
15 physical bonds between polymer chains. Hydrogels absorb water and become fully swollen
16 state, which is common to living tissues in some physical properties (Hamidi, Azadi, & Rafiei,
17 2008). Results related to the influence of LNP (presence and content) on swelling behavior of
18 the PVA/CH hydrogels are presented in **Figure 3c**. The results show that the swelling behav-
19 ior of physically crosslinked hydrogels is influenced by the addition of lignin nanoparticles.
20 Compared with PVA/CH hydrogel, PVA/CH/1LNP exhibited higher and faster swelling rate,
21 until reaching the maximum (856.6 %) after 23 hours (644.2 % for PVA/CH hydrogel). It is
22 axiomatic, since more uniform micropores (Figure 1b) indicates higher affinity for water.
23 However, when the loading of the LNP increased to 3 wt%, the swelling rate reduced, despite
24 a relative more homogeneous pore structure formed. This consequence should be ascribed to
25 the hydrophobic nature of the lignin, which has been confirmed in our previous works
26 (Fortunati et al., 2016; Frigerio, 2014; Weijun Yang et al., 2015). After 23 h, the swelling rate
27 decreased gradually, which was due to the migration and dissolving of some PVA into water.

28 Generally, the swelling property is highly related to the crosslinking degree between the
29 PVA molecules, i.e., the swelling capability will decrease with the increase of the crosslink-
30 ing degree. At the same time, higher crosslinking degree is beneficial to the mechanical prop-

1 erties of the hydrogels (Tong, Zheng, Lu, Zhang, & Cheng, 2007). In this study, it is supposed
2 that the strong interaction between PVA/CH molecules and LNP prevents the PVA molecules
3 from moving and dissolving into the water, resulting in promoting the crosslinking effect.
4 Consequently, more uniform and higher quantity of pore microstructures formed, increasing
5 the swelling property and reinforcing the mechanical behaviours. The schematic diagram has
6 been presented in **Figure 4**. Some other researchers also obtained the common results by
7 adding layered silicates (Xia et al., 2003) and carbon nanotube (Tong et al., 2007) into the
8 hydrogels.



9
10 **Figure 4:** Schematic diagram showing the interactions between PVA/CH molecules and LNP
11 nanoparticles

12

13

14 *3.6 Antiradical activity of migrating substances*

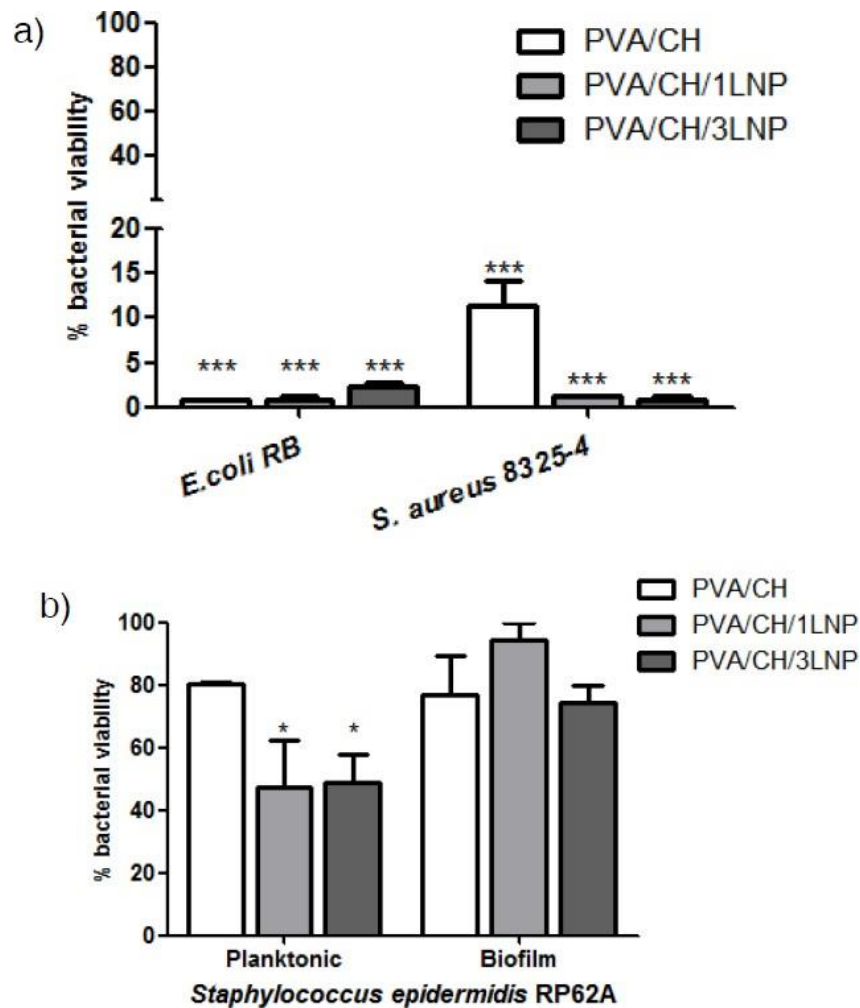
15 **Figure 3d** shows the antioxidant response of migrating substances for different nanocompo-
16 site hydrogels directly immersed into the methanol solution for 24 h. The pure PVA samples

1 were regarded as control samples and did not show any DPPH radical scavenging activity, as
2 expected (not given in curve). When mixing with 10 wt% of chitosan, the absorption value at
3 517 nm of PVA/CH hydrogel decreased to 25.3 from 35.6%, with RSA value of 28.9%, high-
4 lighting a good antioxidation response. Antioxidant properties of chitosan derivatives have
5 been studied (K. W. Kim & Thomas, 2007; Xie, Xu, & Liu, 2001). The scavenging mecha-
6 nism of chitosan is based on the fact that the residual free amino (NH₂) groups can react with
7 free radicals to form stable radicals, afterwards NH₂ groups form ammonium (NH₃⁺) groups
8 by absorbing the hydrogen ions from the solution (Yen, Yang, & Mau, 2008). With the addi-
9 tion of 1 wt % LNP (PVA/CH/1LNP hydrogel), a more remarkable DPPH scavenging activity
10 could be obtained (74.3%, absorption 9.2%). In the hydrogel containing 3 wt % LNP
11 (PVA/CH/3LNP), the antioxidant activity increased up to 78.6% (absorption 7.6%), and the
12 mechanism for antioxidation effect of LNP has been well discussed in our previous study (W.
13 Yang et al., 2016). Lignin nanoparticles can serve as antioxidation controlled release agents in
14 PVA/CH hydrogel.

15

16 3.7 Antibacterial activity

17 Since it was previously reported that lignin extracts (Dong et al., 2011; S. Kim et al., 2013)
18 and LNP (W. Yang et al., 2016) showed antibacterial activity on different bacterial strains, we
19 decided to verify whether LNP affected bacterial growth also upon incorporation into hydro-
20 gels. Therefore, we selected two laboratory strains representing Gram positive and negative
21 classes, i.e. *Staphylococcus aureus* 8325-4 and *Escherichia coli* RB, respectively. We ana-
22 lyzed the effect of the generated hydrogels on the growth of these two strains at 37°C for 24
23 hours, thus in the optimal condition for their growth. As shown in **Figure 5a** a drastic reduc-
24 tion in bacterial viability was observed for both bacterial strains. In the case of *E. coli* the
25 growth is reduced more than 95% compared to the control upon incubation on all three types
26 of nanocomposites (p<0.001). Regarding *S. aureus*, a reduction greater than 85% on PVA/CH
27 blend is observed (p<0.001), whereas on PVA/CH/1LNP and PVA/CH/3LNP the decrease in
28 bacterial survival is even more marked (more than 95%) (p<0.001). These data led us to spec-
29 ulate that already the neat hydrogel bearing CH without LNP may already display an antibac-
30 terial activity.



1
2 **Figure 5:** Bacterial viability of *E. coli* strain RB and *S. aureus* strain 8325-4 on different
3 nanocomposite hydrogels at 37°C for 24 hours (a). Data are presented as viability percentage
4 to TCPs reference set equal to 100%. One-way ANOVA with Bonferroni post-test was per-
5 formed to evaluate statistical significance. All data were compared with TCP reference
6 (**= $p < 0.001$); Bacterial viability of *S. epidermidis* strain RP62A on different nanocomposite
7 hydrogels at 37°C for 24 hours in both planktonic and biofilm-forming conditions (b). Data
8 are presented as viability percentage to TCPs reference set equal to 100%. One-way ANOVA
9 with Bonferroni post-test was performed to evaluate statistical significance. All data were
10 compared with TCP reference (*= $p < 0.05$)

11
12 As a matter of fact, CH has been shown to exert antibacterial activity in different formulations
13 (Dong et al., 2011; S. Kim et al., 2013; Pelgrift & Friedman, 2013), even in the contest of hy-
14 drogels (Abdel-Mohsen et al., 2011). In this case, Abdel-Mohsen and colleagues [9] tested
15 different PVA/CH ratios, showing that the lowest one for CH (80/20) was affecting only *E.*
16 *coli* growth as tested by agar diffusion test. In contrast, our results are slightly different: even
17 if the ratio we used in this study is even lower compared to the one tested by Abdel-Mohsen

1 et al (Abdel-Mohsen et al., 2011), our data suggest that CH may have an effect already alone
2 and LNP nanofilling may have an additive effect, especially on *S. aureus* cells.
3 However, it has to be underlined that we used an assay that measures the metabolic activity of
4 live bacteria, thus being more sensitive than agar diffusion test. Furthermore, the antimicrobi-
5 al activity of the generated hydrogels against *S. epidermidis* RP62A, a coagulase-negative
6 *Staphylococcus* able to form a strong biofilm (Christensen, Baddour, & Simpson, 1987), was
7 evaluated. Therefore, hydrogels affected *S. epidermidis* viability both in planktonic and in
8 biofilm-forming conditions (**Figure 5b**). As shown, a significant ($p < 0.05$) antibacterial action
9 is observed only on LNP-enriched hydrogels in planktonic conditions, instead PVA/CH
10 nanocomposite was not affecting *S. epidermidis* growth. Upon testing of hydrogels efficacy
11 against biofilm formation, none of three blends displayed a significant antibiofilm activity.
12 This reflects the much stronger well-known resistance of biofilm-embedded bacteria to expo-
13 sure to any type of stress. Furthermore, it is noteworthy that the increased concentration of
14 LNP in PVA/CH/3LNP blend reduced bacterial viability, but to level comparable to PVA/CH
15 nanocomposite especially in biofilm-forming conditions for *S. epidermidis* strain. In our cul-
16 ture conditions, both CH and LNP seems to be ineffective against biofilm formation. It may
17 be necessary to increase the content of both components in the nanocomposites in order to be
18 more efficacious. Lastly, the adhesion to the produced hydrogels of all three used bacterial
19 strains was investigated by SEM observation. As reported in **Figure 6**, both staphylococcal
20 strains showed great adherence to the substrate, possibly owing to their many surface adhe-
21 sion proteins (Foster, Geoghegan, Ganesh, & Hook, 2014). Even if SEM images seem to be in
22 contrast with viability assay, we need to point out that microscopy observation does not in-
23 form about viability: bacterial cell are shown attached to the surface but it does not mean that
24 those cells are alive. By contrast, *E. coli* RB showed extremely limited adhesion ability, being
25 almost absent on all three hydrogels indirectly confirming and supporting the data on cell via-
26 bility.
27

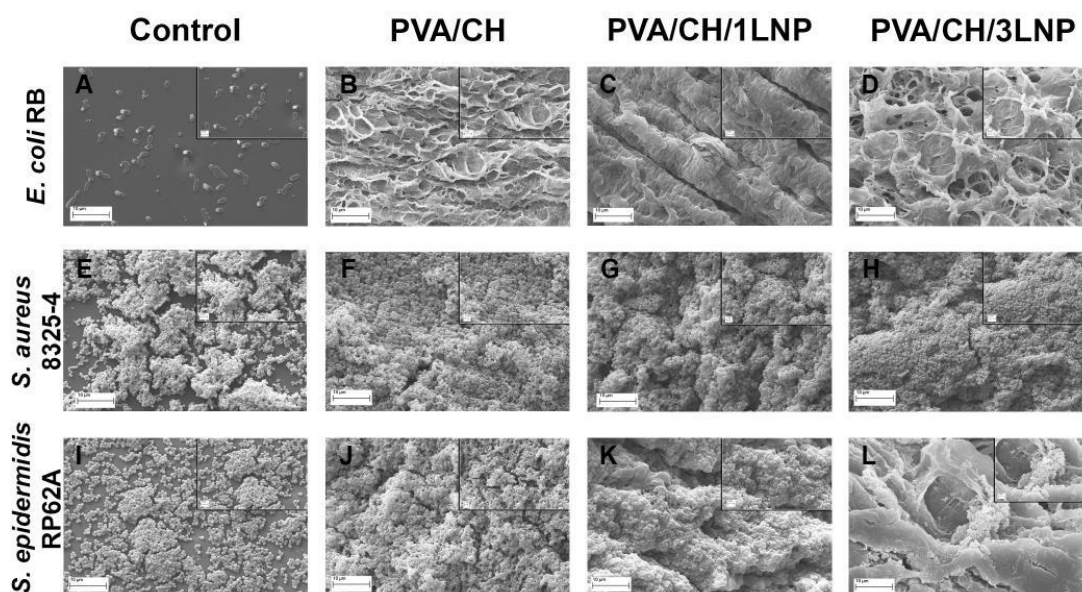


Figure 6: SEM representative images of *E. coli* strain RB (panels B, C and D), *S. aureus* strain 8325-4 (panels F, G and H) and *S. epidermidis* RP62A (panels J, K and L) cultured on the generated LNP-enriched PVA/CH hydrogels for 24 hours at 37°C. Plastic control is also shown for each bacterial strain (panels A, E, I).

4. Conclusions

PVA/CH hydrogels containing 1 and 3 wt% of LNP were successfully prepared by applying a freezing-thawing procedure. It was observed that more uniform and higher porosity (pores with diameter about 10-20 μm), formed in the presence of LNP, facilitated the accessibility of water into the amorphous regions of the hydrogels. The results demonstrated that 1 wt % of LNP could efficiently enhance both the thermal and mechanical properties of PVA/CH hydrogels, due to the strong interactions between PVA/CH and LNP obtained during the applied process, whereas the presence of some agglomerates limited the effect in the case of 3 wt% LNP based formulations. The swelling studies underlined that the strong obtained interaction between PVA/CH molecules and LNP prevents the PVA molecules from moving and dissolving into the water, resulting in promoting the crosslinking effect. Moreover, LNP revealed to be efficient in terms of antioxidative response, serving as release agents in synergism with CH in the PVA/CH. Chitosan and LNP components showed to be also both effective against *E.coli* and *S.aureus* bacteria strain, suggesting the possible use of PVA/CH hydrogels incorporating LNP in biomedical and packaging sectors.

1 **Acknowledgements**

2 W. Yang appreciates the funding support from China Scholarship Council (CSC). The authors
3 also appreciate the Scanning Electron Microscopy (SEM) characterization from Sapienza
4 University of Rome. This research was performed within the framework of TD COST Action
5 TD1305 “Improved Protection of Medical Devices Against Infection (IPROMEDAI)”
6 (http://www.cost.eu/COST_Actions/tdp/TD1305).

7

8 **References**

- 9 - Abdel-Mohsen, A., Aly, A., Hrdina, R., Montaser, A., & Hebeish, A. (2011). Eco-synthesis
10 of PVA/chitosan hydrogels for biomedical application. *Journal of Polymers and the*
11 *Environment*, 19(4), 1005-1012.
- 12 - Bonilla, J., Fortunati, E., Atarés, L., Chiralt, A., & Kenny, J. M. (2014). Physical, structural
13 and antimicrobial properties of poly vinyl alcohol–chitosan biodegradable films. *Food*
14 *Hydrocolloids*, 35, 463-470.
- 15 - Chen, C.-H., Wang, F.-Y., Mao, C.-F., Liao, W.-T., & Hsieh, C.-D. (2008). Studies of
16 chitosan: II. Preparation and characterization of chitosan/poly (vinyl alcohol)/gelatin ternary
17 blend films. *International journal of biological macromolecules*, 43(1), 37-42.
- 18 - Chernoberezhskii, Y. M., Atanesyan, A., Dyagileva, A., Lorentsson, A., & Leshchenko, T.
19 (2002). Effect of the concentration of sulfate lignin on the aggregation stability of its aqueous
20 dispersions. *Colloid Journal*, 64(5), 637-639.
- 21 - Christensen, G. D., Baddour, L. M., & Simpson, W. A. (1987). Phenotypic variation of
22 *Staphylococcus epidermidis* slime production in vitro and in vivo. *Infect Immun*, 55(12),
23 2870-2877.
- 24 - Cotana, F., Cavalaglio, G., Nicolini, A., Gelosia, M., Coccia, V., Petrozzi, A., & Brinchi, L.
25 (2014). Lignin as co-product of second generation bioethanol production from
26 ligno-cellulosic biomass. *Energy Procedia*, 45, 52-60.
- 27 - Crini, G., & Badot, P.-M. (2008). Application of chitosan, a natural aminopolysaccharide, for
28 dye removal from aqueous solutions by adsorption processes using batch studies: A review of
29 recent literature. *Progress in Polymer Science*, 33(4), 399-447.
- 30 - Domenek, S., Louaifi, A., Guinault, A., & Baumberger, S. (2013). Potential of lignins as
31 antioxidant additive in active biodegradable packaging materials. *Journal of Polymers and the*
32 *Environment*, 21(3), 692-701.
- 33 - Dong, X., Dong, M., Lu, Y., Turley, A., Jin, T., & Wu, C. (2011). Antimicrobial and
34 antioxidant activities of lignin from residue of corn stover to ethanol production. *Industrial*
35 *Crops and Products*, 34(3), 1629-1634.
- 36 - Fortunati, E., Yang, W., Luzi, F., Kenny, J., Torre, L., & Puglia, D. (2016). Lignocellulosic
37 nanostructures as reinforcement in extruded and solvent casted polymeric nanocomposites: an
38 overview. *European Polymer Journal*, 80, 295-316.
- 39 - Foster, T. J., Geoghegan, J. A., Ganesh, V. K., & Hook, M. (2014). Adhesion, invasion and
40 evasion: the many functions of the surface proteins of *Staphylococcus aureus*. *Nat Rev*

1 *Microbiol*, 12(1), 49-62.

2 - Frigerio, P. (2014). Biopolymers in elastomers: lignins as biofiller for tyre compound.
3 Università degli Studi di Milano-Bicocca.

4 - Hamidi, M., Azadi, A., & Rafiei, P. (2008). Hydrogel nanoparticles in drug delivery.
5 *Advanced Drug Delivery Reviews*, 60(15), 1638-1649.

6 - Hu, X.-Q., Ye, D.-Z., Tang, J.-B., Zhang, L.-J., & Zhang, X. (2016). From waste to
7 functional additives: thermal stabilization and toughening of PVA with lignin. *RSC Advances*,
8 6(17), 13797-13802.

9 - Kai, D., Tan, M. J., Chee, P. L., Chua, Y. K., Yap, Y. L., & Loh, X. J. (2016). Towards
10 lignin-based functional materials in a sustainable world. *Green Chemistry*.

11 - Kim, K. W., & Thomas, R. (2007). Antioxidative activity of chitosans with varying
12 molecular weights. *Food chemistry*, 101(1), 308-313.

13 - Kim, S., Fernandes, M. M., Matamá, T., Loureiro, A., Gomes, A. C., & Cavaco-Paulo, A.
14 (2013). Chitosan–lignosulfonates sono-chemically prepared nanoparticles: Characterisation
15 and potential applications. *Colloids and Surfaces B: Biointerfaces*, 103, 1-8.

16 - Kim, S. J., Park, S. J., & Kim, S. I. (2003). Swelling behavior of interpenetrating polymer
17 network hydrogels composed of poly (vinyl alcohol) and chitosan. *Reactive and Functional*
18 *Polymers*, 55(1), 53-59.

19 - Korbag, I., & Mohamed Saleh, S. (2016). Studies on the formation of intermolecular
20 interactions and structural characterization of polyvinyl alcohol/lignin film. *International*
21 *Journal of Environmental Studies*, 1-10.

22 - Kubo, S., & Kadla, J. F. (2003). The formation of strong intermolecular interactions in
23 immiscible blends of poly (vinyl alcohol)(PVA) and lignin. *Biomacromolecules*, 4(3),
24 561-567.

25 - Kumar, M. N. R. (2000). A review of chitin and chitosan applications. *Reactive and*
26 *Functional Polymers*, 46(1), 1-27.

27 - Lee, L. J., Zeng, C., Cao, X., Han, X., Shen, J., & Xu, G. (2005). Polymer nanocomposite
28 foams. *Composites Science and Technology*, 65(15–16), 2344-2363.

29 - Liu, P., Chen, W., Liu, Y., Bai, S., & Wang, Q. (2014). Thermal melt processing to prepare
30 halogen-free flame retardant poly (vinyl alcohol). *Polymer Degradation and Stability*, 109,
31 261-269.

32 - Pallavicini, P., Dona, A., Taglietti, A., Minzioni, P., Patrini, M., Dacarro, G., . . . Visai, L.
33 (2014). Self-assembled monolayers of gold nanostars: a convenient tool for near-IR
34 photothermal biofilm eradication. *Chemical Communications*, 50(16), 1969-1971.

35 - Pelgrift, R. Y., & Friedman, A. J. (2013). Nanotechnology as a therapeutic tool to combat
36 microbial resistance. *Adv Drug Deliv Rev*, 65(13-14), 1803-1815.

37 Rinaudo, M. (2006). Chitin and chitosan: Properties and applications. *Progress in Polymer*
38 *Science*, 31(7), 603-632.

39 - Saino, E., Sbarra, M. S., Arciola, C. R., Scavone, M., Bloise, N., Nikolov, P., Visai, L.
40 (2010). Photodynamic action of Tri-meso (N-methyl-pyridyl), meso (N-tetradecyl-pyridyl)
41 porphine on *Staphylococcus epidermidis* biofilms grown on Ti6Al4V alloy. *The International*
42 *journal of artificial organs*, 33(9), 636-645.

43 - Sbarra, M. S., Arciola, C. R., Di Poto, A., Saino, E., Rohde, H., Speziale, P., & Visai, L.
44 (2009). The photodynamic effect of tetra-substituted N-methyl-pyridyl-porphine combined

1 with the action of vancomycin or host defense mechanisms disrupts *Staphylococcus*
2 *epidermidis* biofilms. *The International journal of artificial organs*, 32(9), 574-583.

3 - Slaughter, B. V., Khurshid, S. S., Fisher, O. Z., Khademhosseini, A., & Peppas, N. A. (2009).
4 Hydrogels in regenerative medicine. *Advanced Materials*, 21(32 - 33), 3307-3329.

5 - Taglietti, A., Arciola, C. R., D'Agostino, A., Dacarro, G., Montanaro, L., Campoccia, D.,
6 Pallavicini, P. (2014). Antibiofilm activity of a monolayer of silver nanoparticles anchored to
7 an amino-silanized glass surface. *Biomaterials*, 35(6), 1779-1788.

8 - Tang, Y.-F., Du, Y.-M., Hu, X.-W., Shi, X.-W., & Kennedy, J. F. (2007). Rheological
9 characterisation of a novel thermosensitive chitosan/poly(vinyl alcohol) blend hydrogel.
10 *Carbohydrate Polymers*, 67(4), 491-499.

11 - Thakur, V. K., Thakur, M. K., Raghavan, P., & Kessler, M. R. (2014). Progress in green
12 polymer composites from lignin for multifunctional applications: a review. *ACS Sustainable*
13 *Chemistry & Engineering*, 2(5), 1072-1092.

14 - Tong, X., Zheng, J., Lu, Y., Zhang, Z., & Cheng, H. (2007). Swelling and mechanical
15 behaviors of carbon nanotube/poly (vinyl alcohol) hybrid hydrogels. *Materials Letters*, 61(8),
16 1704-1706.

17 - Xia, X., Yih, J., D'Souza, N. A., & Hu, Z. (2003). Swelling and mechanical behavior of poly
18 (N-isopropylacrylamide)/Na-montmorillonite layered silicates composite gels. *Polymer*,
19 44(11), 3389-3393.

20 - Xie, W., Xu, P., & Liu, Q. (2001). Antioxidant activity of water-soluble chitosan derivatives.
21 *Bioorganic & Medicinal Chemistry Letters*, 11(13), 1699-1701.

22 - Yalcinkaya, E. E., Puglia, D., Fortunati, E., Bertoglio, F., Bruni, G., Visai, L., & Kenny, J. M.
23 (2017). Cellulose nanocrystals as templates for cetyltrimethylammonium bromide mediated
24 synthesis of Ag nanoparticles and their novel use in PLA films. *Carbohydr Polym*, 157,
25 1557-1567.

26 - Yang, J. M., Su, W. Y., Leu, T. L., & Yang, M. C. (2004). Evaluation of chitosan/PVA
27 blended hydrogel membranes. *Journal of Membrane Science*, 236(1-2), 39-51.

28 Yang, J. M., Su, W. Y., & Yang, M. C. (2004). Evaluation of chitosan/PVA blended hydrogel
29 membranes. *Journal of Membrane Science*, 236(1), 39-51.

30 Yang, W., Fortunati, E., Dominici, F., Giovanale, G., Mazzaglia, A., Balestra, G. M., Puglia,
31 D. (2016). Effect of cellulose and lignin on disintegration, antimicrobial and antioxidant
32 properties of PLA active films. *Int J Biol Macromol*, 89, 360-368.

33 - Yang, W., Kenny, J. M., & Puglia, D. (2015). Structure and properties of biodegradable
34 wheat gluten bionanocomposites containing lignin nanoparticles. *Industrial Crops and*
35 *Products*, 74, 348-356.

36 - Yang, X., Liu, Q., Chen, X., Yu, F., & Zhu, Z. (2008). Investigation of PVA/ws-chitosan
37 hydrogels prepared by combined γ -irradiation and freeze-thawing. *Carbohydrate Polymers*,
38 73(3), 401-408.

39 - Ye, D.-z., Jiang, L., Hu, X.-q., Zhang, M.-h., & Zhang, X. (2016). Lignosulfonate as
40 reinforcement in polyvinyl alcohol film: Mechanical properties and interaction analysis.
41 *International journal of biological macromolecules*, 83, 209-215.

42 - Yen, M.-T., Yang, J.-H., & Mau, J.-L. (2008). Antioxidant properties of chitosan from crab
43 shells. *Carbohydrate Polymers*, 74(4), 840-844.

44 - Zu, Y., Zhang, Y., Zhao, X., Shan, C., Zu, S., Wang, K., . . . Ge, Y. (2012). Preparation and

- 1 characterization of chitosan–polyvinyl alcohol blend hydrogels for the controlled release of
- 2 nano-insulin. *International journal of biological macromolecules*, 50(1), 82-87.
- 3